

# Synthesis and Characterization of a “Turn-On” photoCORM for Trackable CO Delivery to Biological Targets

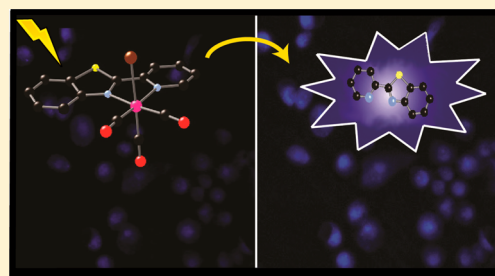
Samantha J. Carrington,<sup>†</sup> Indranil Chakraborty,<sup>†</sup> Jenna M. L. Bernard,<sup>‡</sup> and Pradip K. Mascharak<sup>\*,†</sup>

<sup>†</sup>Department of Chemistry and Biochemistry, University of California, Santa Cruz, California 95064, United States

<sup>‡</sup>Department of Chemistry, University of California, Berkeley, California 94720, United States

## Supporting Information

**ABSTRACT:** A designed photoactive CO releasing molecule (photoCORM), namely, *fac*-[MnBr(CO)<sub>3</sub>(pbt)] (**1**, pbt = 2-(2-pyridyl)-benzothiazole), promotes CO-induced death of MDA-MB-231 human breast cancer cells upon illumination with broadband visible light. The CO release from this photoCORM can be tracked by rise in fluorescence within the cellular matrix due to deligation of the pbt ligand. The results of this study suggest the potential of **1** in eradication of cancer cells through CO delivery.



**KEYWORDS:** Carbon monoxide, photoactive metal carbonyls, CO delivery, apoptosis, fluorescence tracking

The surprising discovery of salutary effects of low concentrations of carbon monoxide (CO) in mammalian physiology has shifted the paradigm of signaling molecules in biology.<sup>1</sup> This noxious gas is endogenously produced through the catabolism of heme cofactor by the enzyme heme oxygenase (HO)<sup>2</sup> and plays a key role in various cytoprotective pathways.<sup>3–5</sup> For example, low concentrations (<200 ppm) of CO have been shown to provide protection against ischemic reperfusion injury<sup>6,7</sup> and improve organ/graft survival rates in animal models.<sup>8,9</sup> The difficulties associated with handling CO gas in hospital settings, however, limit its use as a therapeutic, a fact that prompted the quest for CO-releasing molecules (or CORMs) for CO delivery to biological targets.<sup>10–13</sup> Because larger ( $\geq 300$  ppm) doses of CO causes shutdown of respiration and release of cyt c from the mitochondrial membrane which in turn initiates apoptotic cascades through caspase activation,<sup>2</sup> it is now apparent that the outcome of CO delivery could vary drastically depending on the doses of CO delivered to a biological target. Compared to normal cells, the proapoptotic effect of CO is more prominent in aggressive T cell, dysregulated hyperproliferative smooth muscle cells, and cancer cells.<sup>11</sup> As a consequence, CO sensitizes cancer cells to chemotherapy as well as induces apoptosis in prostate, colon, and other cancer cells.<sup>14,15</sup> These findings have led to the realization that if delivered selectively CO could destroy malignant cells, many of which often exhibit resistance to common chemotherapeutics. In order to achieve control on CO delivery, we<sup>16–18</sup> and others<sup>19–21</sup> have developed photoactive metal carbonyl complexes (photoCORMs) that could be triggered by illumination with lights of suitable wavelengths. These photoCORMs have allowed CO delivery to eradicate malignant cells under the control of light. For example, Schatzschneider and co-workers have reported CO-induced

eradication of HT29 colon cancer cells with a Mn-based photoCORM [Mn(CO)<sub>3</sub>(tpm)]<sup>+</sup> (tpm = tris(pyrazolyl)-methane, illumination at 365 nm),<sup>22</sup> while we have recently demonstrated very efficient dose-dependent eradication of MDA-MB-231 (human breast cancer cells) and HeLa cells with the photoCORM *fac*-[MnBr(azpy)(CO)<sub>3</sub>] (azpy = 2-(phenyl)-azopyridine) under visible light.<sup>23</sup>

The success in eradication of malignant cells via light-triggered CO delivery from designed photoCORMs requires proper tracking of the CO donors within cellular matrixes. In order to make our photoCORMs *trackable in biological targets*, we have now synthesized a fluorescent metal carbonyl complex that acts as a “turn-on” photoCORM. This Mn carbonyl complex, namely, *fac*-[MnBr(CO)<sub>3</sub>(pbt)] (pbt = 2-(2-pyridyl)-benzothiazole), is sensitive to visible light and displays enhancement of fluorescence upon CO release. This phenomenon has been realized through fluorescence imaging studies with MDA-MB-231 human breast cancer cell line. Ford and co-workers have recently reported a trackable photoCORM, namely, [Re(bpy)(CO)<sub>3</sub>(thp)] (where thp = tris(hydroxymethyl) phosphine), which changes its emission wavelength upon CO photorelease (illumination at 405 nm) within PPC-1 human prostatic carcinoma cells.<sup>24</sup> However, no apparent toxicity or cell death has been reported with this photoCORM.

The complex *fac*-[MnBr(CO)<sub>3</sub>(pbt)] (**1**) was synthesized by the reaction of [MnBr(CO)<sub>5</sub>] and pbt in equimolar ratio in dichloromethane at room temperature (see the Supporting Information for details). X-ray quality crystals of **1** were

**Received:** October 2, 2014

**Accepted:** November 17, 2014

**Published:** November 17, 2014

obtained by layering hexanes over its dichloromethane solution. The X-ray crystal structure of complex **1** is shown in Figure 1.

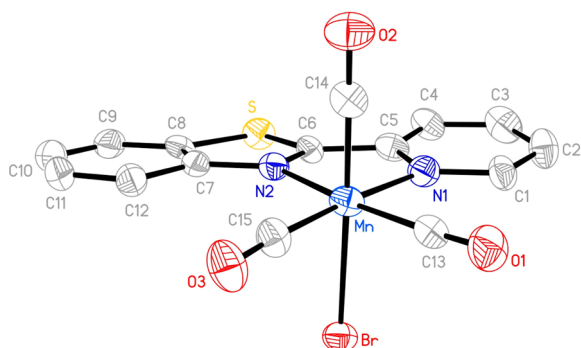


**Figure 1.** Molecular structure of *fac*-[MnBr(CO)<sub>3</sub>(pbt)] (**1**). Thermal ellipsoids are shown at 50% probability level, and the hydrogen atoms are omitted for clarity. Selected bond distances (Å) Mn–Br, 2.5254(15); Mn–C13, 1.792(9); Mn–C14, 1.768(9); Mn–C15, 1.779(9); Mn–N1, 2.077(7); Mn–N2, 2.055(6).

The Mn(I) center resides in a distorted octahedral coordination sphere with three CO ligands in a facial disposition. The Mn–Br distance in **1** (2.5254(15) Å) is comparable to that in the corresponding bpy complex [MnBr(bpy)(CO)<sub>3</sub>] (2.538(10) Å).<sup>25</sup> The Mn–CO bond lengths of **1** are also comparable to those observed with the bpy complex [MnBr(bpy)(CO)<sub>3</sub>].

When kept in the dark, solutions of **1** in DMSO, dichloromethane, acetonitrile, DMSO–water, DMSO–phosphate buffer, and acetonitrile–water mixtures exhibit prolonged stability (as monitored by spectrophotometry). The electronic absorption spectra of complex **1** in these solvents and solvent–water mixtures exhibit two absorption bands (Figure 2). The

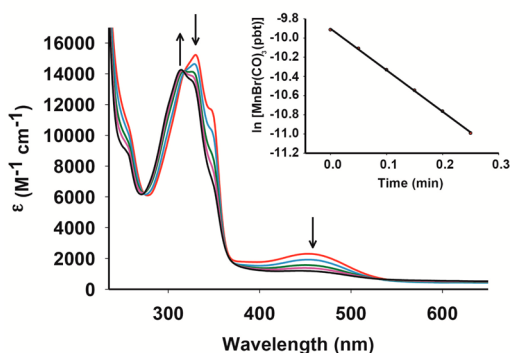


**Figure 2.** Spectral changes of **1** in dichloromethane solution upon exposure to broadband visible light (10 mW/cm<sup>2</sup>, with a 440 nm cutoff filter).

low-energy band in the 400–500 nm region presumably arises from a metal-to-ligand charge transfer (MLCT) transition.<sup>23,25</sup> When exposed to low power (10–15 mW) visible light, solutions of **1** exhibit sequential changes (Figure 2) characteristic of CO photorelease.<sup>23,25,26</sup> The release of CO from **1** upon illumination has been confirmed by reduced myoglobin (Mb) assay (see Supporting Information).

In the present work, the apparent rates of CO photorelease ( $k_{\text{CO}}$ ) of **1** have been determined in various solvent systems. When measured in dichloromethane with a 440 nm cutoff filter, **1** exhibits a  $k_{\text{CO}}$  value of  $4.32 \pm 0.01 \text{ min}^{-1}$  (conc.  $1.021 \times 10^{-4}$

M), while in acetonitrile solution, a modest drop is observed ( $1.05 \pm 0.01 \text{ min}^{-1}$ , conc.  $1.03 \times 10^{-4}$  M). Appreciable solubility of **1** in acetonitrile–water (40:60, v/v) and DMSO–water (20:80 v/v) mixtures allows its use in biological studies. The former mixture was used for the cellular imaging, while the latter was employed for cell viability studies. In such mixed solvent systems, moderately slow  $k_{\text{CO}}$  values are observed. For example, in acetonitrile–water mixture, the  $k_{\text{CO}}$  drops to  $0.23 \pm 0.01 \text{ min}^{-1}$  (conc.  $1.62 \times 10^{-4}$  M), while in DMSO–water mixture, a value of  $0.61 \pm 0.01 \text{ min}^{-1}$  (conc.  $1.39 \times 10^{-4}$  M) is noted with a 400 nm cutoff filter. Despite such slow down, one must note that the rates of CO photorelease from **1** are still considerably “fast” compared to other photoCORMs reported in the literature.<sup>19–21</sup>

The choice of the pbt ligand in the present work stems from two specific characteristics of this benzothiazole derivative. First, this ligand is a stable fluorophore that displays strong emission at 390 nm. Second, it exhibits strong antitumor activities much like other benzothiazoles.<sup>27</sup> Interestingly, complex **1** shows a weak emission band centered at 390 nm upon excitation at 330 nm. However, when a solution of **1** in acetonitrile–water (40:60 v/v) mixture was exposed to eight consecutive 30 s pulses of visible light (15 mW), a 20-times enhancement in luminescence intensity was observed (Figure 3). Comparison of the ninth trace (black) with that of free pbt

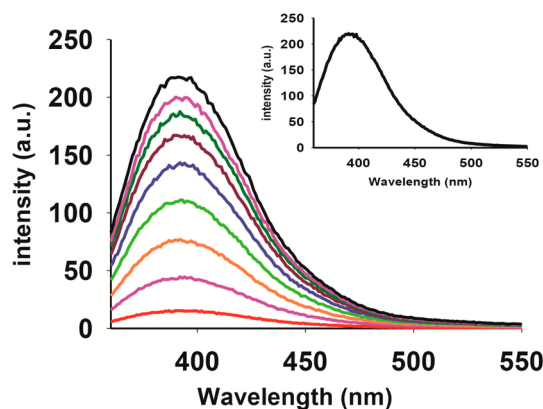


**Figure 3.** Time-dependent enhancement of emission intensity ( $\lambda_{\text{em}}$ , 390 nm) for **1** in acetonitrile–water (40:60 v/v) mixture upon exposure to visible light (excitation wavelength 330 nm). Concentration of **1** =  $1.16 \times 10^{-4}$  M. The inset displays the emission spectrum of free pbt ligand (concentration =  $1.16 \times 10^{-4}$  M).

ligand (inset of Figure 3) of the same concentration (conc.  $1.16 \times 10^{-4}$  M) indicated that this trace corresponds to free pbt ligand in solution. It is therefore evident that loss of CO from **1** upon exposure to visible light also causes deligation of the pbt ligand, a step that is responsible for the “turn-on” event.

The concomitant loss of the pbt ligand from **1** during photorelease of CO in acetonitrile–water mixtures raised questions regarding the nature of the Mn-containing species left in the photolyzed solutions in air. We have addressed this issue with the aid of X-band EPR spectroscopy. The X-band EPR spectrum (at 77 K) of the photolyzed solution of **1** exhibits a six line spectrum (Figure 4 top) indicative of a Mn(II) species. The Mn(II) center in such solution appears to exist as an acetonitrile complex, and the modest hyperfine broadening possibly arises from ligand exchange (Br<sup>−</sup>) as reported by Chan and co-workers.<sup>28</sup> This is corroborated by the fact that a

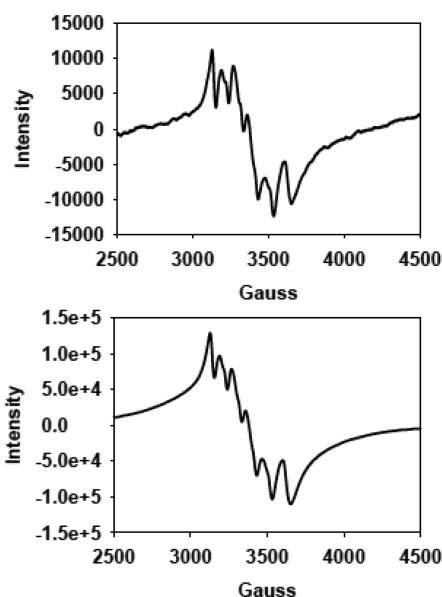


**Figure 4.** X-band EPR spectra (at 123 K) of the photolyzed solution of complex **1** in acetonitrile–water (40:60 v/v) solution (50  $\mu$ M, top) and  $\text{MnSO}_4$  + KBr mixture in acetonitrile–water (40:60 v/v) solution (100  $\mu$ M, bottom). Microwave frequency, 9.44 GHz; modulation amplitude, 2.00 G; and modulation frequency, 100 kHz.

solution of  $\text{MnSO}_4$  with equimolar KBr in acetonitrile–water (40:60, v/v) mixture also affords a very similar EPR spectrum (Figure 4 bottom). The close resemblance of these two EPR spectra suggests that upon photolysis the Mn(I) center of **1** undergoes oxidation to Mn(II) and remains as a solvated species in solution. It is also important to note that, when the photolyzed solution was evaporated to dryness and the residue was subjected to IR spectroscopy, the solid displayed no CO stretch in the entire 1700–3000  $\text{cm}^{-1}$  region. Moreover, the most prominent IR bands observed were those arising from the free pbt ligand, which further supports the findings of the fluorescence experiment. Taken together, these results strongly suggest that upon illumination **1** rapidly releases three CO ligands and eventually the bidentate pbt ligand, leaving a solvated Mn(II) species and free pbt in the photolyzed solution. The 20-times enhancement of the fluorescence intensity upon photolysis (as shown in Figure 3) arises from the free pbt.

The overall behavior of **1** under illumination made it clear to us that this photoCORM could serve as a “turn-on” CO donor that displays luminescence upon CO delivery to cellular targets. To demonstrate such applicability, we performed fluorescence-imaging studies with MDA-MB-231 human breast cancer cells. The cells were incubated for 2 h with 50  $\mu$ M of **1** after which the media was carefully aspirated. Following a wash cycle, the cells were placed in PBS buffer and the suspension was mounted on a Zeiss AxioObserver Z1 microscope (fitted with Hamamatsu 9100-13 EMCCD camera) without fixing. The fluorescence images were then recorded at  $t = 0$  (Figure 5a) and after three 10 s illumination pulses of visible light (Figure 5b). The bright “turn-on” fluorescence displayed by the cells after illumination reveals that CO loss from **1** indeed results in release of free pbt. Close examination of the cells in Figure 5b,c reveals the presence of free pbt ligand within the cells.

The rapid internalization of **1** in the MDA-MB-231 cancer cells and subsequent release of CO and the pbt ligand (with strong antitumor properties) upon illumination prompted us to

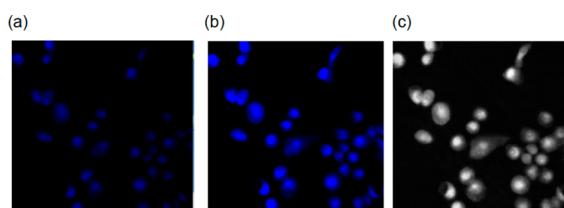


**Figure 5.** Fluorescence images of MDA-MB-231 cells incubated with 50  $\mu$ M complex **1** for 2 h at 37  $^{\circ}$ C ( $\lambda_{\text{exc}}$  350 nm;  $\lambda_{\text{em}}$  390 nm; short pass DAPI filter cube). (a) First image without light exposure, (b) image recorded after three 10 s pulses of low power LED light, and (c) gray scale version of image (b).

examine the possibility of eradication of such cells under the control of visible light. Following the addition of **1**, colonies of MDA-MB-231 cells ( $1 \times 10^4$  per well) in 96-well plates were exposed to visible light for 45 min and incubated for an additional 20 min in the dark. Next, the wells were carefully aspirated to remove the media along with the photoproduct(s). After addition of fresh media, the cells were further incubated in the dark for 4 h. The viability of the cells was finally assessed by MTT assay. As shown in Figure 6, a dose-dependent killing

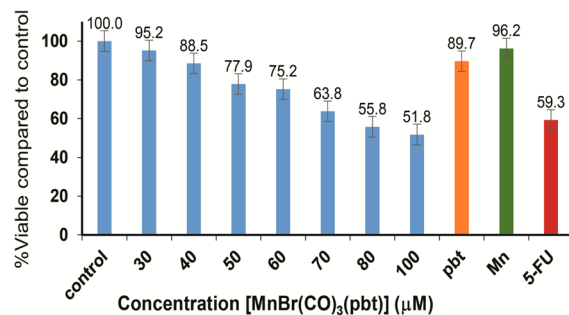


**Figure 6.** Dose dependent cell viability of MDA-MB-231 (blue bar) cells upon treatment with CO photoreleased from **1**. The orange and green bars represent the cell viability upon treatment with 100  $\mu$ M PBT and  $\text{MnSO}_4$ , respectively, and the red bar indicates the cell viability with 5-fluorouracil (25  $\mu$ M). All samples were illuminated with a broadband visible light.

of the cancer cells was observed (done in triplicate). Approximately 50% reduction in viability was observed with 100  $\mu$ M **1** under visible light illumination. This efficacy compares well with the extent of cell kill by 25  $\mu$ M of 5-fluorouracil (5-FU) upon incubation for 72 h. It is important to note that the control experiment with  $\text{MnSO}_4$  at the highest concentrations (100  $\mu$ M) showed almost no reduction in cell viability. However, incubation with a similar concentration of pbt caused minor reduction in cell viability in line with its antitumor properties. Finally, the dark control experiment with **1** showed insignificant cell death even at the highest concentration (100  $\mu$ M) employed in the light experiments. These findings collectively indicate that the present photoCORM **1** promotes rapid CO-induced apoptosis in MDA-MB-231 cells under the control of light. In our earlier work, another photoCORM *fac*-[ $\text{MnBr}(\text{azpy})(\text{CO})_3$ ] reduced the cell viability to a similar extent ( $\sim 55\%$  at 80  $\mu$ M). However, the present photoCORM allowed us to track the entry of the CO donor into the cells (Figure 5a) and the event of CO photorelease by fluorescence enhancement (Figure 5b) due to release of pbt in the cytosol.

In summary, the results of the present study demonstrate that the photoCORM **1** (a) can deliver CO to biological targets with the aid of very low power visible light, (b) can promote rapid CO-induced apoptosis in MDA-MB-231 human breast cancer cells, and (c) the highly fluorescent pbt offers a unique way to track the CO delivery within the cells as revealed from the cellular imaging experiments. To our knowledge, **1** is the first “turn-on” photoCORM that allows one to track CO delivery in cellular matrixes. We anticipate that designed carbonyl complexes of this kind could be employed to deliver controlled doses of CO to eradicate malignant cells that otherwise exhibit resistance to regular chemotherapeutics.

## ■ ASSOCIATED CONTENT

### Supporting Information

Details regarding experimental procedure, and spectroscopic and crystallographic parameters. This material is available free of charge via the Internet at <http://pubs.acs.org>.

### Accession Codes

The CCDC deposition number for the crystal structure is 1026066.

## ■ AUTHOR INFORMATION

### Corresponding Author

\*E-mail: [pradip@ucsc.edu](mailto:pradip@ucsc.edu).

### Notes

The authors declare no competing financial interest.

## ■ ACKNOWLEDGMENTS

Financial support from the NSF grant DMR-140933 is gratefully acknowledged. We thank Dr. Steven Ruzin (Department of Plant and Microbial Biology, University of California, Berkeley) for help with the cellular imaging experiments and Graham Roseman (Department of Chemistry and Biochemistry, University of California, Santa Cruz) for help with EPR measurements.

## ■ REFERENCES

- (1) Kim, H. P.; Rytter, S. W.; Choi, A. M. K. CO as a cellular signaling molecule. *Annu. Rev. Pharmacol. Toxicol.* **2006**, *46*, 411–49.
- (2) Kikuchi, G.; Yoshida, T.; Noguchi, M. Heme oxygenase and heme degradation. *Biochem. Biophys. Res. Commun.* **2005**, *338*, 558–567.
- (3) Stein, A. B.; Bolli, R.; Dawn, B.; Sanganalmath, S. K.; Zhu, Y.; Wang, O.-L.; Guo, Y.; Motterlini, R.; Xuan, Y.-T. Carbon monoxide induces a late preconditioning-mimetic cardioprotective and anti-apoptotic milieu in the myocardium. *J. Mol. Cell. Cardiol.* **2012**, *52*, 228–236.
- (4) Queiroga, C. S. F.; Tomasi, S.; Wideroe, M.; Alves, P. M.; Vercelli, A.; Vieira, H. L. A. Preconditioning triggered by carbon monoxide (CO) provides neuronal protection following perinatal hypoxia-ischemia. *PLoS One* **2012**, *7*, e42632.
- (5) Zeynalov, E.; Doré, S. Low doses of carbon monoxide protect against experimental focal brain ischemia. *Neurotoxic. Res.* **2009**, *15*, 133–137.
- (6) Stein, A. B.; Guo, Y.; Tan, W.; Wu, W.-J.; Zhu, X.; Li, Q.; Luo, C.; Dawn, B.; Johnson, T. R.; Motterlini, R.; Bolli, R. Administration of a CO-releasing molecule induces late preconditioning against myocardial infarction. *J. Mol. Cell. Cardiol.* **2005**, *38*, 127–134.
- (7) Tulis, D. A.; Keswani, A. N.; Peyton, K. J.; Wang, H.; Schafer, A. I.; Durante, W. Local Administration of carbon monoxide inhibits neointima formation in balloon injured rat carotid arteries. *Cell. Mol. Biol.* **2005**, *51*, 441–446.
- (8) Nakao, A.; Choi, A. M. K.; Murase, N. Protective effect of carbon monoxide in transplantation. *J. Cell. Mol. Med.* **2006**, *10*, 650–671.
- (9) Sato, K.; Balla, J.; Otterbein, L.; Smith, R. N.; Brouard, S.; Lin, Y.; Choi, A. M.; Bach, F. H.; Soares, M. P. Carbon monoxide generated by heme oxygenase-1 suppresses the rejection of mouse-to-rat cardiac transplants. *J. Immunol.* **2001**, *166*, 4185–4194.
- (10) Heinemann, S. H.; Hoshi, T.; Westerhausen, M.; Schiller, A. Carbon monoxide-physiology, detection and controlled release. *Chem. Commun.* **2014**, *50*, 3644–3660.
- (11) Motterlini, R.; Otterbein, L. E. The therapeutic potential of carbon monoxide. *Nat. Rev. Drug Discovery* **2010**, *9*, 728–743.
- (12) Romao, C. C.; Blättler, W. A.; Seixas, J. D.; Bernardes, G. J. L. Developing drug molecules for therapy with carbon monoxide. *Chem. Soc. Rev.* **2012**, *41*, 3571–3583.
- (13) Alberto, R.; Motterlini, R. Chemistry and biological activities of CO-releasing molecules (CORMs) and transition metal complexes. *Dalton Trans.* **2007**, 1651–1660.
- (14) Wegiel, B.; Gallo, D.; Csizmadia, E.; Harris, C.; Belcher, J.; Vercellotti, G. M.; Penacho, N.; Seth, P.; Sukhatme, V.; Ahmed, A.; Pandolfi, P. P.; Helczynski, L.; Bjartell, A.; Persson, J. L.; Otterbein, L. E. Carbon monoxide expedites metabolic exhaustion to inhibit tumor growth. *Cancer Res.* **2013**, *73*, 7009–7021.
- (15) Song, R.; Zhou, Z.; Kim, P. K. M.; Shapiro, R. A.; Liu, F.; Ferran, C.; Choi, A. M. K.; Otterbein, L. E. Carbon monoxide promotes Fas/CD95-induced apoptosis in jurkat cells. *J. Biol. Chem.* **2004**, *279*, 44327–44334.
- (16) Heilman, B. J.; Gonzalez, M. A.; Mascharak, P. K. Photoactive metal nitrosyl and carbonyl complexes derived from designed auxiliary ligands: an emerging class of photochemotherapeutics. *Prog. Inorg. Chem.* **2014**, *58*, 185–224.
- (17) Chakraborty, I.; Carrington, S. J.; Mascharak, P. K. Design strategies to improve the sensitivity of photoactive metal carbonyl complexes (photoCORMs) to visible light and their potential as CO-donors to biological targets. *Acc. Chem. Res.* **2014**, *47*, 2603–2611.
- (18) Gonzales, M. A.; Mascharak, P. K. Photoactive metal carbonyl complexes as potential agents for targeted CO delivery. *J. Inorg. Biochem.* **2014**, *133*, 127–135.
- (19) Rimmer, R. D.; Pierri, A. E.; Ford, P. C. Photochemically activated carbon monoxide release for biological targets. Toward developing air-stable photoCORMs labilized by visible light. *Coord. Chem. Rev.* **2012**, *256*, 1509–1519.
- (20) Schatzschneider, U. PhotoCORMs: Light-triggered release of carbon monoxide from the coordination sphere of transition metal complexes for biological applications. *Inorg. Chim. Acta* **2011**, *374*, 19–23.
- (21) Crespy, D.; Landfester, K.; Schubert, U. S.; Schiller, A. Potential photoactivated metallopharmaceuticals: from active molecules to supported drugs. *Chem. Commun.* **2010**, *46*, 6651–6662.
- (22) Niesel, J.; Pinto, A.; Peindy N'Dongo, H. W.; Merz, K.; Ott, I.; Gust, R.; Schatzschneider, U. Photoinduced CO release, cellular uptake and cytotoxicity of a tris(pyrazolyl)methane (tpm) manganese tricarbonyl complex. *Chem. Commun.* **2008**, 1798–1800.
- (23) Carrington, S. J.; Chakraborty, I.; Mascharak, P. K. Rapid CO release from Mn(I) carbonyl complex derived from azopyridine upon exposure to visible light and its phototoxicity toward malignant cells. *Chem. Commun.* **2013**, *49*, 11254–11256.
- (24) Pierri, A. E.; Pallaoro, A.; Wu, G.; Ford, P. C. A luminescent and biocompatible PhotoCORM. *J. Am. Chem. Soc.* **2012**, *134*, 18197–18200.
- (25) Chakraborty, I.; Carrington, S. J.; Mascharak, P. K. Photo-delivery of CO by designed photoCORMs: Correlation between absorption in the visible region and metal-CO bond labilization in carbonyl complexes. *ChemMedChem* **2014**, *9*, 1266–1274.
- (26) Gonzalez, M. A.; Carrington, S. J.; Fry, N. L.; Martinez, J. L.; Mascharak, P. K. Syntheses, structures and properties of new manganese carbonyls as photoactive CO-releasing molecules: design strategies that lead to CO photolability in the visible region. *Inorg. Chem.* **2012**, *51*, 11930–11940.

- (27) Xie, X.; Yan, Y.; Zhu, N.; Liu, G. Benzothiazoles exhibit broad-spectrum antitumor activity: their potency, structure-activity and structure-metabolism relationships. *Eur. J. Med. Chem.* **2014**, *76*, 67–78.
- (28) Chan, S. I.; Fung, B. M.; Lütje, H. Electron paramagnetic resonance of Mn(II) complexes in acetonitrile. *J. Chem. Phys.* **1967**, *47*, 2121–2130.